International Journal of Scientific Research & Engineering Trends
Volume 6, Issue 5, Sept-Oct-2020, ISSN (Online): 2395-566X

Autonomous UV Sanitization Robot with Social Distancing, Body Temperature and Mask Detection Using Automatic Path Planning and Multi-Terrain Capabilities

Aryan Mehta
Dept of Mechanical Engineering
VeermataJijabai Technological Institute, Matunga, Mumbai,
aryanmehta2610@gmail.com,

Mohan Kshirsagar
Sinhgad Institute of Technology Lonavala
k94mak@gmail.com

Reetu Jain
reetu.jain@onmyowntechnology.com

Shekhar Jain
shekhar.jain@onmyowntechnology.com

***Abstract*-With the outbreak of the infectious coronavirus disease development of new norms and rules in every country have been taken. Wearing a mask and implementing social distancing along with frequent sanitization of public areas is of utmost necessity during this worldwide health crisis. Subsequently, officials have been appointed roles to monitor the extent and ensure the effective compliance of the new guidelines by the general public. However, it would be very difficult for humans to correctly administer this for a prolonged period of time. Moreover, this would not only pose a threat to the public, but also affect the person conducting the screening process. In an attempt to find a solution to this issue, the proposed autonomous UV sanitization robot has a complete utility based design which helps in detecting social distancing and the wearing of masks using image processing. Thermal imaging is also utilised to detect whether a person is suffering from a fever. The main feature of this design is to provide complete sanitization using ultraviolet light as a disinfectant by a process known as ultraviolet germicidal irradiation (UVGI). Special rotating outward flaps containing UV tube lights increase the range of disinfection to higher areas on walls and even extend to ceilings. A bell drive mechanism forms the locomotive basis defining the mobility of the robot. Rotating flippers have been connected to the shafts of the main wheels which help dynamically manoeuvre the robot. Its multi-terrain capabilities make it versatile enough to be deployed in various public places including hospitals, malls, shopping centres, parks, and even on the road. With thorough simulative experimentation, impressive results have been obtained which help achieve the main aim of this study.**

***Keywords*-COVID-19, Coronavirus, Social distancing, Sanitization, UV lights, Multi-terrain.**

I.INTRODUCTION

With the inception of COVID-19, through the various months, countries have established certain laws and restraints on the movement of people to prevent the increase in the number of infected cases. Despite immense effort the surge in cases is steady with a proportionate mortality rate. The basic plan involved implementing an extremely strict lockdown followed by the gradual ease of these restrictions with the aim of slowing down the rate of spread and buying time while several healthcare organizations, scientists and medical experts try to develop a vaccine. Social distancing is a globally implemented practice which refers [1] to a non-pharmaceutical infection prevention and control intervention implemented to avoid/decrease contact between those who are infected with the disease causing pathogen and those who are not, so as to stop or slow down the rate and extent of disease transmission in a community. This eventually leads to decrease in spread, morbidity and mortality due to the disease. According to WHO [2], it is prescribed to have a safe distance of at least 6 feet (approximately 2 meters) between each other in orderto correctly implement social distancing. Although most people are consciously making an effort to socially distance themselves and wear masks, only a few are being able to do so with considerable effectiveness. Consequently, violations of social distancing and wearing a mask in public need to be extensively monitored and kept a check on. This calls on for a better and more accurate method of monitoring using image processing which can efficiently identify violations and thus prevent spread. The drastic increase in the influx of patients in hospitals make it very difficult for them to manage and tend to the needs of all. Regular sanitization every day becomes mandatory along with increasing use of sanitizers in every room, hallway, and passage. Likewise,

all public places have to follow this regimented set of tasks to help contain the virus. The major source of spread is through physical contact, either directly or through walls, surfaces, poles and frequently touched objects such as door handles, lift buttons, money bills, parcels and so on. Considerable time and workforce are required to repeat the same job over and over again, which, instead of preventing the spread, might actually increase it.

UV light has been used for sterilization and disinfection as early as the mid-20th century. For the specific need of the hour, UV light disinfection is being increasingly used as a means of sanitization since ultraviolet (UV) treatment process is an extremely quick physical process. UV sterilization also known [3] as UV disinfection or ultraviolet germicidal irradiation (UVGI) works by breaking down certain chemical bonds and scrambling the structure of DNA, RNA and proteins, causing a microorganism to be unable to multiply. When a microorganism is unable to multiply, it is considered dead since it cannot reproduce within a host and is no longer infectious. Thus, it serves as a reliable method of sanitization.

Motivated by this, the authors of this work are attempting to create a well-designed robot which aims to serve as an efficient aid to humans by almost avoiding physical contact as a whole. A defined structure of placing UV lights has been arranged to cover maximum area of sanitization. Its autonomous capabilities rule out the need for people to continuously control it and direct it. Identification of social distancing and the wearing of masks is accurate and dependable. This robot along with its multiple features poses as an 'ALL IN ONE' project and would considerably decrease human contact thus helping us not only battle the pandemic but also pose as a model for various purposes with futuristic utility.

II. RELATED WORK AND BASIC DESCRIPTION

The utilization of novel technology is ever increasing. The current times demand for innovation in the smallest form possible. New designs are being developed on a frequent basis trying to accommodate different forms technology, both hardware oriented and software oriented. The pandemic has stimulated plenty of research papers striving to present the best solution to this gigantic crisis. The field of robotics is undergoing continuous transition with new ideas and designs emerging from all over the world. It is important to adopt a practical approach having a balance between the number of features, size, material, and aesthetics in order to aid humans in the best possible way.

A research paper published on 6th May, 2020 on the monitoring of social distancing [4] using fine-tuned YOLO and Deep-sort techniques primarily focuses on social distancing which is an important method of controlling the spread of COVID-19. Similar researchpapers implementing various other methods of control are being published. An integration of a few of these methods of spread control accommodated in the form of a single versatile robot could serve as a very efficient and practical solution. This is the main aim of the study.

Countries such as India and South Korea [5] [6] [7], for example, are adopting GPS tracking technologies to point out locations of infected people in order to avoid them from exposing themselves to healthy people. The Indian government has worked and developed the AarogyaSetu App, which locates any infected person in the surrounding area using GPS and Bluetooth along with monitoring social distancing helping keep a recommended distance from one another [8].

In this research, we have utilized a bell drive mechanism for the ground movement of the robot which allows the robot to move in rough as well as smooth terrain. Flippers surrounded by conveyor belts have been attached to all four wheels which help turn the robot smoothly in all directions. The basal assembly of the robot has an intricate design utilizing various gears, shafts and sliding plates. A LIDAR sensor has been placed on the front side for object detection. In the upper assembly, a hexagonal shaped design has been used with rotating flaps alternately placed to cover maximum area of sanitization. The outward movement and inclination of flaps containing the UV lights are being controlled by a linear actuator present in the interiors of the robot. Two cameras are required to be placed on top of the robot – one for sensory objectives and the detection of social distancing and wearing of masks and the second for thermal imaging to identify a person suffering from a fever. Amalgamating all of these technologies into a single design helps us achieve a versatile robot which can dynamically manoeuvre itself.

III. OUR SOLUTION – ROBOT MODEL PARTS AND MECHANISMS

The design of the proposed robot will be extensively described in this section. A basic layout of the design would include the basal assembly, the upper assembly and the electronics used. The robot is almost symmetrical with a few minor differences on both sides, hence it has a relatively easy understanding of its construction and working.

1. Basal Assembly

The base contains all the parts responsible for the locomotion of the robot. For multi-terrain purposes a flipper mechanism has been adopted on both, the front and the back side. The main wheels have conveyor belts running along the left and right side connecting the front and back wheels on either side. The flipper mechanism

has each flipper containing two wheels connected using conveyor belts in a similar fashion as described earlier. There are a total of 4 flippers, each being connected to a single main wheel via a shaft. Due to the height of the upper assembly, it is important to have a robust base which can manage to keep the centre of gravity of the whole robot as low as possible. A LIDAR has been fixed on the front side for object detection to manoeuvre past obstacles.

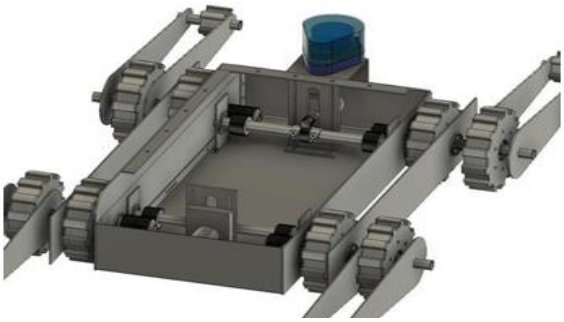

Fig: 1 Basal Assembly**.**

2. Upper Assembly

The upper portion of the robot rests on the base of the robot and consists of a hexagonal design. Each face of the hollow hexagonal prism contains an inward cavity to provide space for the installation of the UV lights. The upper assembly is divided into 2 levels with 2 UV lights per face on the first level and 1 UV light per face on the second level. The edge length of the second level is smaller than the first and each alternate face of the hexagon in the second level consists of a rotating flap exactly fitting in the cavity. Each flap, containing a UV light, is rotated by the linear actuator along its hinge joint, allowing the UV light to sanitize elevated levels on the targeted surface. The interior portion contains the linear actuator from which the 3 arising shafts are connected to the flaps. A common mount is placed on the top of the upper assembly toaccommodate the two cameras which can also move. The desired material used to build the upper assembly is aluminium as it has a low density, and is very malleable thus allowing easier machining and manufacture.

Fig: 2 Upper Assembly.

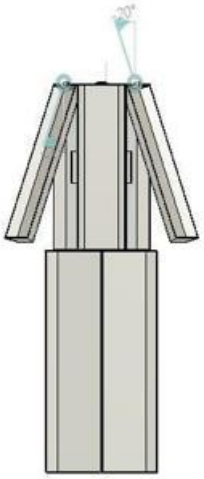

Fig: 3 (C).

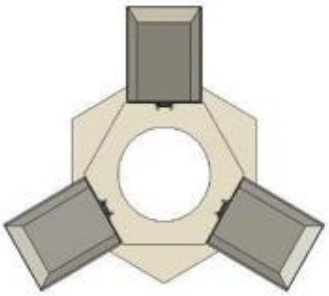

Fig: 4 (D).

IV. LINEAR ACTUATOR

The linear actuator is situated on the top of the upper assembly with its embedded working mechanism exposed to the viewer, while the hub of links extending from the actuator and connecting to the shafts of the UV flaps are hidden within the hollow assembly. Here, linear motion is being converted into rotary motion to allow the UV flaps to open outwards as shown in figure E. The designed angle for maximum sanitization by the emitted UV Light is 20 degrees outwards. This value of rotary displacement can easily be achieved with any good grade linear actuator.

Fig: 5 Linear Actuator.

V. INTERNAL DRIVING MECHANISM

The internal mechanism utilized in this design is very intricate and constantly transfers motion from one form to another. The internal mechanism is placed within the basal assembly hence it is not visible when in operation. The front axle and the back axle of the robot have the same working and containing mechanical parts arranged in the same fashion. The larger motor, able to translate along the sliding plate, is meshed with a helical gear via its pinion gear.

Fig: 6 Internal driving mechanism.

The helical transfers its motion on both sides to ultimately make the shaft of its main wheel rotate. Both the main wheels on each side are connected usingconveyor belts which are in contact with the ground. When the conveyor belts move in the same direction the robot translates linearly and when they move in the opposite direction the robot changes direction. Thelayout of the parts is visible in Figure A and Figure F.

1. Electronics

1.1. Sensors:
Our sensory requirements include a LIDAR for 3-D mapping of robot path and several Infrared Strip Sensors of touch sensing to avoid obstacles in its path. The LIDAR model has been placed on the front side of the basal assembly while the infrared sensor arrays will be present on all 4 sides.

Specifications required for LIDAR:
- Total Diameter Range: Approximately 12m
- Angular Range: 0-360 degrees
- Distance Resolution: < 0.5mm
- Angular Resolution: <= 1 degrees
- Sample Duration: 0.5ms
- Sample Frequency: 2000 – 2010Hz
- Scan Rate: 1 ~ 10Hz, Typical 5.5Hz

To meet the specific requirements, an apt selection for the model of LIDAR would be [9] A1M8 360 Degree Laser Range Finder – 12m.
Specifications required for Touch Sensors:
- Distance measuring range: 4 cm to 30 cm
- Output type: Analog voltage
- Output voltage differential over distance range: 2.05 V (typical)
- Update period: 38 ± 10 ms

To meet the specific requirements, we would choose 8 pieces of Infrared Sensor model - GP2Y0A41SK0F [10] to be placed on all sides of the base.

1.2. Motors:
A robust set of motors is required to drive the composite mesh of gears leading to the wheels and eventually connecting the flippers. 6 motors are required to drive the four main wheels.
Specifications required for the larger motor:
- Base Motor RPM: 18000
- Operating Voltage: 6-18 V
- Rated Voltage: 12 V
- Rated Torque: 34.2 N-cm
- Stall Torque: 300 N-cm
- Gearbox Dimensions: 25×37 (L x W) mm

Specifications for the smaller motor:
- Rated current (mA): ≤3600

- Rated power (W): 7.836
- Rated Torque (N-cm): 77.4

Rated speed: 90 RPM Shaft length (mm): 27 Shaft diameter (mm): 8 Base motor RPM: 6000

2 Identical 12V 300 RPM Johnson Geared DC motors [11] and 4 identical MG555 12V 100RPM Square Gearbox DC motors [12] are suitable, matching the above criteria well within limits. These motors are simple DC motors coupled with a metal gearbox for delivering more torque.

1.3. Motor Driver:
3 motor drivers are required to run the 6 motors used in the assembly. It should be able to change the speed of the motor using a potentiometer. Switching directions of rotation of the motor is also a necessary requirement in the motor driver. Specifications of the motor driver:
- Maximum Motor Current - Continuous: 10 A
- Maximum Motor Current - Peak (Less than 10 seconds): 30 A
- Internal PWM Generator Frequency: 9 ~ 11 kHz

An appropriate selection for the above specifications is the MD10-POT Motor Driver [13] as it is designed to enable the speed to be controlled via a potentiometer (10K Ohm). A 3-way rocker switch is used for start/stop and direction control.

1.4. Central Processing Unit (CPU):
A CPU would be required for the processing of all the operations, ranging from physical locomotive commands to image processing commands. The operations are quite heavy and to process them with increased response speed, a high quality CPU would be necessary.

Specifications of the processor: - The 10th Generation Intel® Core™ i7 Processor i7-10710U 4.7GHz, 6 core [14] is an example of a high quality CPU capable of processing all the functions smoothly with negligible lag time.

1.5. Ultraviolet Lights (UV):

The UV lights are strategically placed in the first on the second level of the upper assembly in order to achieve maximum area of sanitization. We have placed 12 UV on the first level of the assembly, 2 oneach face of the hexagon while on the second level, there are a total of 6 UV lights, 1 on each face of the hexagon. The lower level is designed for keeping 12 UV lights of 20W power each and the second level has 6 UV lights of 8W power each. On the second level there are outward rotating flaps hinged at their top edge, alternately placed which can open outward to a maximum angle of 20 degrees to sanitize higher portions on walls and cover areas on ceilings too.

20W UV Lights:

Specifications:

- Useful Life: 11000 hr
- Lamp Wattage: 20 W
- Lamp Voltage: 45 V
- Lamp Current: 0.450 A
- UV-C Radiation: 6.0 W Product Dimensions
- Reference Length A: 398 (max) mm
- Insertion Length B: 402.7 (min), 405.1 (max) mm
- Overall Length C: 412.2 (max) mm
- Diameter D: 16 (max) mm

An example of a suitable UV light, both in specifications and size, would be the Philips TUV 20W FAM TL Mini [15]. They offer almost constant UV output over their complete lifetime, for maximum security of disinfection and high system efficacy

8W UV Lights:

Specifications:

- Useful Life: 11000 hr
- Lamp Wattage: 8 W
- Lamp Voltage:56 V
- Lamp Current: 0.15 A
- UV-C Radiation: 2.4 W

Product Dimensions:

- Reference Length A: 283.3 (max) mm
- Insertion Length B: 293 (min), 295.4 (max) mm
- Overall Length C: 302.5 (max) mm
- Diameter D: 16 (max) mm

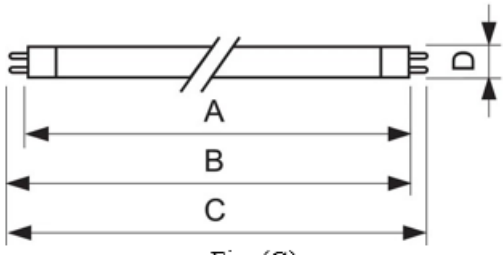

Fig: 7 Ultraviolet Lights.

An example of a suitable UV light, both in specifications and size, would be the Philips TUV 8W FAM TL Mini (1 Foot) [16]. They offer almost constant UV output over their complete lifetime, for maximum security of disinfection and high system efficacy

1.6. Current Requirements:

The Basal Assembly consists of the following current requirements for specific parts:

Larger Motor: 3.6A; Smaller Motor: 2.5A; LIDAR: 1A, 5V; 6 Touch Sensors: 200mA, 5V

On a single side, 2 smaller motors and 1 larger motor are connected

According to Kirchhoff's Current Law (KCL) which is Kirchhoff's first law [17], it deals with the conservation of charge entering and leaving a junction. His current law states that for a parallel path the total current entering a circuit junction is exactly equal to the total current leaving the same junction. Algebraic sum of ALL the currents entering and leaving a junction must be equal to zero as:

$\Sigma I_{IN} = \Sigma I_{OUT}$

Hence, total current requirements would be the addition of all individual device current requirements. Current requirements by motors on one side = (2 x 2.5 A) + 3.6 A = 8.6A

Therefore, current requirements by motors on both side = (2 x 8.6 A) = 17.2A

Total Basal Assembly Current requirements = Current required by LIDAR + Current required by 6 Touch Sensors + current required by motors on both sides = 17.2 + 1 + 0.2 = 18.4 A

The Upper Assembly consists of the following current requirements for specific parts:

Linear Actuator: 3A, 12V; Cameras: 1A (approx...) Total current requirements would be the addition of all individual device current requirements

Total Current requirements of Upper Assembly = 3 + 1 = 4A (approx...)

1.7. Interfacing

The CPU or the central processing unit is the main server which congregates inputs from all parts of the robot. The following flowchart describes the network of the robot as a whole. On the left side we have 3 branches of inputs. The first one starts with the LIDAR and the infrared sensors connected to the controller via the signal conditioning circuit inputting data into theCPU. The second branch consists of the motors operated by the motor drivers which give information to the CPU via the controller. The 3rd branch, consisting of the cameras – the action camera as well as the thermal camera, have their own circuitry leading to the CPU hence it is independent of the other branches and does not require the controller. The input tasks are simultaneously processed in the CPU with different time frames and lag periods.

The CPU is run by the Robot Operating System (ROS) and shown in the box below the CPU box in the given flowchart. The communication section is branched into 3 modes of communication shown on the right of the CPU box. The CPU can be communicated to via all 3 modes which are Radio Frequencies, Bluetooth and WIFI.

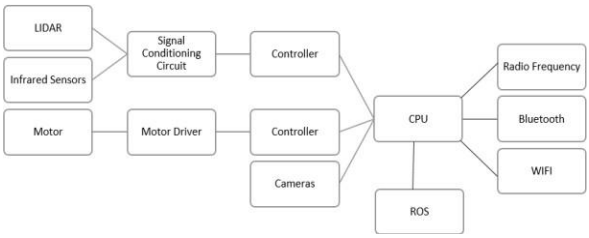

Fig: 8 interfacing.

VI. CODING ALGORITHMS:

1. Face Mask Detection:

The objective of this section is to identify the person on image/video stream wearing face mask with the help of computer vision and deep learning algorithm by using the PyTorch library.

A code should be written on python, which uses specific libraries in order to achieve the above mentioned objective. However, this section explains the steps involved and the algorithm used in the form of a comprehensive flowchart to provide a visual understanding of the procedure.

1.1. Data at Source:

The raw images used for the current study were downloaded from PyImageSearch article and the majority of the images were augmented by OpenCV. The set of images were already labelled “mask” and “no mask”. The images that were present were of different sizes and resolutions, probably extracted from different sources or from machines (cameras) of different resolutions.

1.2. Data Pre-processing:

Pre-processing steps as mentioned below have been applied to all the raw input images to convert them into clean versions, which could be fed to a neural network machine learning model.

- Resizing the input image (256 x 256)
- Applying the colour filtering (RGB) over the channels (Our model MobileNetV2 supports 2D 3 channel image)
- Scaling / normalizing images using the standard mean of PyTorch build in weights
- Centre cropping the image with the pixel value of 224x224x3
- Finally converting them into tensors (Similar to NumPy array)

1.3. Deep Learning Frameworks:

1.3.1. Algorithm:

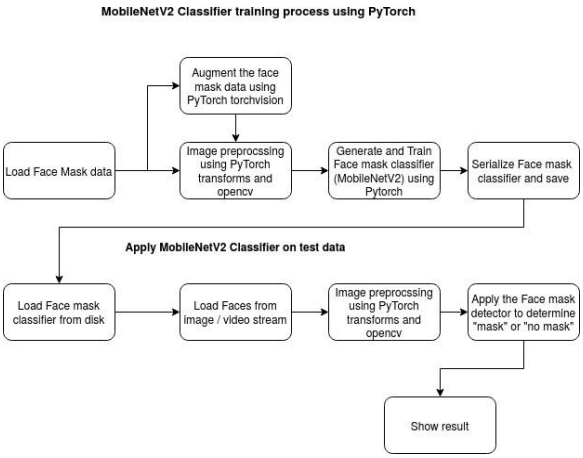

Fig: 9 deep learingframwork.

We are using the PyTorch because it runs on Python, which means that anyone with a basic understanding of Python can get started on building their deep learning models and also it has the following advantage compared with TensorFlow 1. Data Parallelism 2. It looks like a Framework.

1.3.2. Result:

Fig: 10 result.

2. Social Distancing Detection:

A clear understanding of the importance of social distancing and its benefits have been established in the introduction of this paper. Here we are dealing with the procedure involved in measuring social distancing from our robot using image processing constituting a special library called OPENCV.

2.1. Result:

Fig: 11 social distancing detection.

2.2. Algorithm:

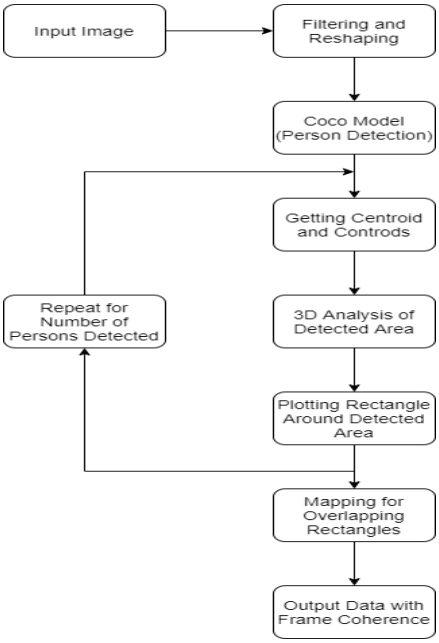

Fig: 12algorithms.

3. Thermal Body Temperature Detection:

The face detection algorithm has been shown previously in this paper. This module is more focused on the algorithm to find the Continuous Body Temperature and calculations required during the procedure of finding the forehead temperature.

3.1. Flowchart:

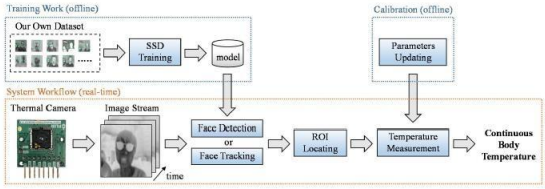

Fig: 13 thermal body temperature detection.

3.2. Calculation of the Temperature:

The Planck's Curve [18] defines the relation between the linear-flux signals and the scene temperature:

$$S = \int_{\lambda_1}^{\lambda_2} \frac{2\pi hc^2}{\lambda^5} \frac{1}{\exp(\frac{hc}{\lambda k T_k}) - 1} R(\lambda) \cdot \delta\lambda$$

Where S refers to the output signal, the spectral band is defined by λ1 and λ2, h being the Planck's constant, c refers to the velocity of light, the Boltzmann's constant is denoted by k, R(λ) is the camera responsivity and the absolute temperature in kelvin is denoted by Tk.

The approximation of the above formula to be used in codes is the following:

$$S = \frac{R}{\exp\left(\frac{B}{T_k}\right) - F} + O$$

Where R, B, F, O are generated parameters during calibration. Making Tk the subject of the equation, we get:

$$T_k = \frac{B}{\ln\left(\frac{R}{S - O} + F\right)}$$

The general values of the generated parameters F and B are 1 and 1428 respectively. From this it is possible to calculate by fitting a linear regression line. The values of R (camera responsiveness) and O (offset) from the regression line are 231159.5 and 6094.248 respectively. Plugging them in the above formula we get:

$$T = \frac{1428}{\ln\left(\frac{231159.5}{S - 6094.248} + 1\right)} - 273.15$$

Where S is the Output Signal and T is our calculated skin temperature. Thus we have managed to calculate the forehead temperature which is equal to the value of the skin temperature T.

4. Path Planning Algorithm:

A free segment is considered as the distance between two endpoints of two different obstacles. It searches the endpoint of a safe segment where the mobile robot turns around this point without hitting obstacles. [19] Algorithm:

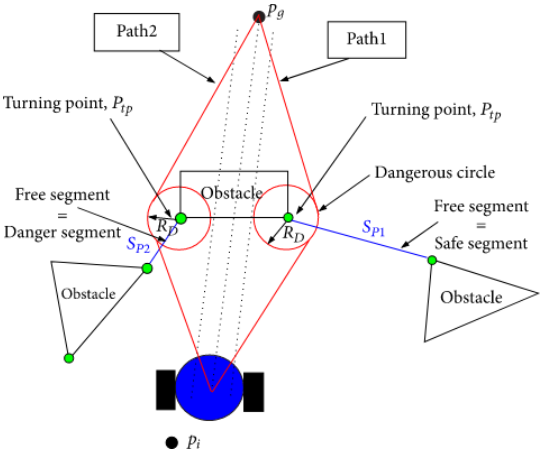

Fig: 14 path planning algorithms.

When there are no obstacles, the path planning problem does not arise. In fact, the robot moves from an initial position to a goal position in a straight line which will be considered as the shortest path. However, when the mobile robot encounters obstacles as shown in Figure, the robot should be turning without collision with obstacles. So, the major problem is how to determine a suitable path from a starting point to a target point in a static environment. To solve this problem our developed algorithm is proposed to search for a turning point of a safe free segment which gives the shortest path and

allows the robot to avoid obstacles. Once the turning point is located, a dangerous circle with radius is fixed in this point. In this case, our proposed strategy aims to search for the turning point of the safe free segment around which the robot turns safely.

For ensuring safety, we select the segment whose distance( ) is larger than the robot diameter with a margin for security( ). On the other hand, the segment whose distance is smaller than the robot diameter is considered as a danger segment. In this work, we take into account only safe segments and danger segments are ignored. Furthermore, and to determine the shortest path, we have determined the point of the safest segment which gives the shortest path. Then a dangerous circle is fixed at this point and the robot turns and moves towards the tangential direction to this circle. Even when there is a danger problem, our proposed algorithm will be reactive to allow the robot to avoid obstacles and reach the goal. In this case, therobot reserves the determined turning point and searches for a new turning point to avoid collision with obstacles. To more clarify our strategy, the different notions of the algorithm are incorporated in Figure and the basic principle is summarized in a flowchart presented in Figure.

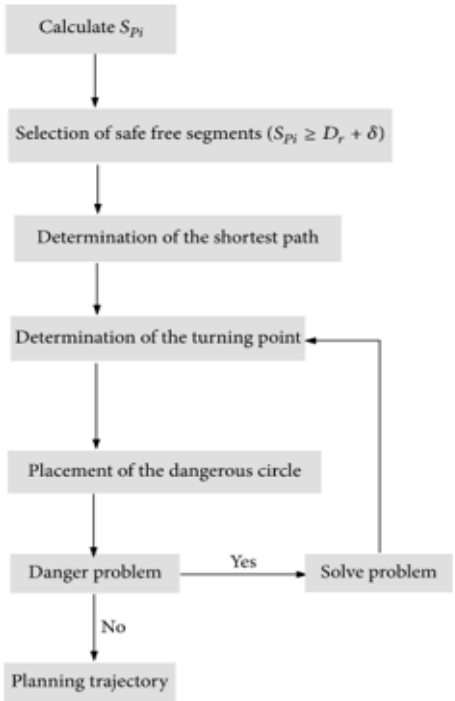

Fig: 15 flowchart.

Current Supply Conversions and Calculations for UV Lights:

5. DC – AC Conversion:

As ultraviolet light requires AC-Current supply and hence it is important to convert the DC power into continuous AC supply in order to be able to efficiently operate the UV lights. Given in Figure O is the conversion flowchart necessary for constant AC supply.

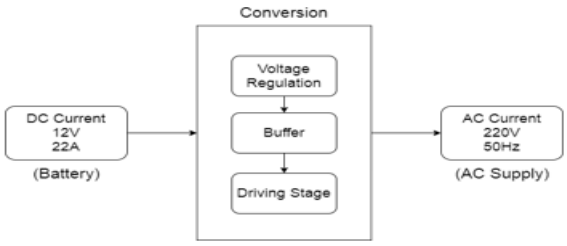

Fig: 16 AC-DC conversion.

VII. EXPOSURE TIME

Just like any other light, even UVC light gets dimmer and dimmer, the farther you move away from the source. The reduction in intensity or power-drop happens very quickly. The simple formula for how fast this energy drops is calculated by power divided by the resultant quantity of distance away from the source raised to the second power (Ed = P/(d^2).

Of all the coronaviruses in the family, the SARS Coronavirus (Urbani) [20] needs the most amount of intensity of the D90 dose of 241 J/m2 to be considered dead or rendered ineffective. The D90 dose of UVC ensures 90% inactivation of all Bacteria and viruses present.

Calculation:

Exposure time = (Desired UV dose) * 4 *pi * (UV bulb distance) 2 / (UV bulb power)

Desired UV dose = 241 J/m2 for

UV bulb distance = Assume 2 or 1.5 meters (approximately 6.5 or 5 feet respectively)

UV bulb power = 20W

Substituting these values in the above formula of exposure time, we get:

Exposure time (2m distance) = approximately 606 seconds = approximately 10 minutes

Exposure time (1.5m distance) = approximately 341seconds = approximately 5 mins 41 seconds

The design has 2 UV lights of 20W Power placed beside each other per face of the hexagon

Therefore, the intensity is considered to be increased by 60%, reducing the exposure by approximately 40%, therefore

Exposure Time = approximately 6 minutes Exposure Time = approximately 3.5 minutes Above are the exposure times for a normal sized

room (16 by 16 feet). Thus the sanitization process is quick and efficient.

VIII. CENTRE OF GRAVITY

A vehicle's centre of gravity, or CG, is the theoretical point where the sum of all of the masses of each of its individual components effectively act. In other words,

from a physics perspective, a vehicle behaves like its entire weight resides at this one point (this is why, in physics class, this is where all forces and moments that are acting on a body are applied). Carrying weight up high, such as a panoramic sunroof will raise a vehicle's CG while placing heavy subsystems low in a vehicle, such as a battery pack, will work to lower it. Lower isbetter from a handling standpoint, as it reduces weight transfer during cornering and braking, and it also reduces the propensity to roll over.

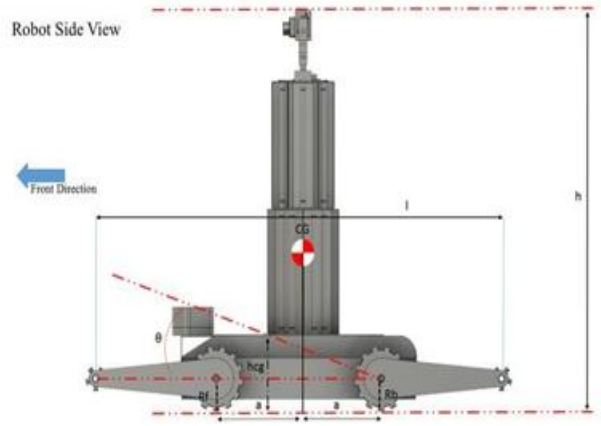

Fig: 17 (Q).

Fig: 18 (R).

We start by measuring the hub heights (RF and RR in the formula below) and weighing the car on level ground (W). Knowing the wheelbase (ℓ) and weight distribution, we can calculate the longitudinal location (a and b) of the centre of gravity (CG). Then we blatantly ignore every safety warning on our lift to set the rear wheels onto homemade platforms and weigh the front axle (WF) in this tilted position. The angle (θ) can be computed using the triangle formed by the wheelbase and the height the rear wheels are raised.Plugging all of this into the following formula spits out CG height

1.Simulation of Static Stresses using constraints:

1. Static Stress on Basal Assembly:

A static stress analysis shown in Figure Q was conducted to see a considerable load act on the basal assembly. The aim of this simulation is to find out the static stress distribution caused by a vertical load placed uniformly on the top face of the assembly. In this specific simulation we have kept the value of load equal to 100N. The various colours on the bar signify whether the assembly is able to support the load without failure. The colours ranging from blue to yellow signify that the portion of the assembly is safe and as we move to red, it has a reduced ability to withstand the load, indicating a possibility of failure. The maximum deflection as specified in the picture is2.303 * 10-6 mm. Thus the deflection caused is negligible. It is clear from the visual analysis that the whole assembly is, more or less quite safe in spite of a high static load, hence there is no need to worry about failure. It would be able to withstand almost everything that generally would occur in its environment.

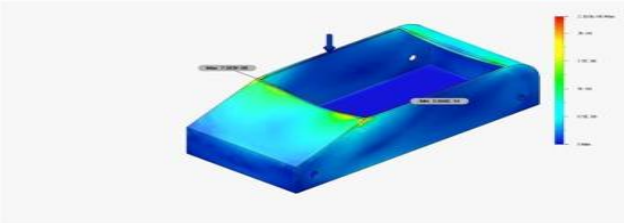

Fig: 19 (S)

2. Static Stress on Upper Assembly:

A similar static stress analysis was conducted on the upper assembly. For the upper assembly it was necessary to apply both horizontal and vertical loads as per what we assume might most accurately represent the distribution of loads in a real life environment.First we have isolated the vertical load with a value of 10N force, a particularly high value to test theassembly with, as compared to what actually might occur. The Figure R shows that the distributed load causes a maximum of 4.188 * 10-4 mm. This value is well within safe limits and hence would allow the assembly to bear substantial vertical load.

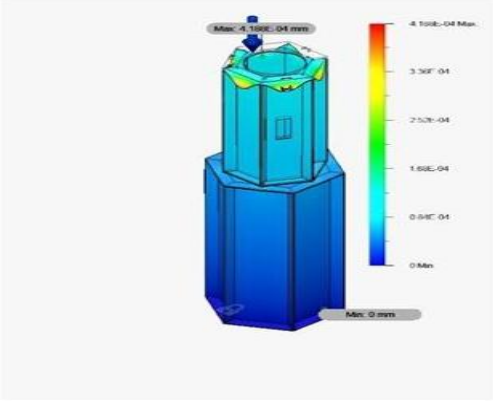

Fig: 20 (T).

The second simulation of static stress analysis shown in Figure S included horizontal loads too along with vertical loads. The horizontal stress mostly comprises stress caused due to forces of compression, hence the usage of compressional loads in the simulation. Here we notice that the maximum deflection caused is equal to 1.76 * 10-4 mm, indicating that the assembly is able to withstand the high static resultant force with negligible deflection.

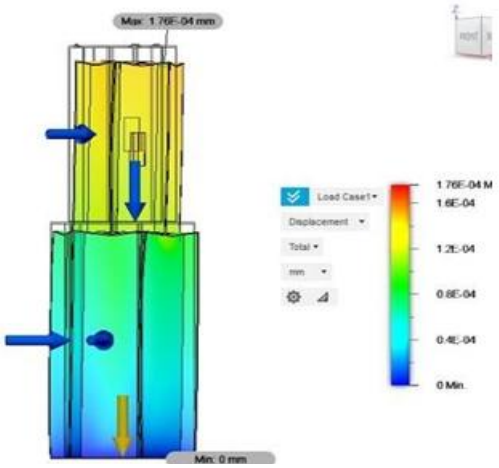

Fig: 21 (U).

3. Robot Design & Dimensions: Upper Assembly:

Top View:

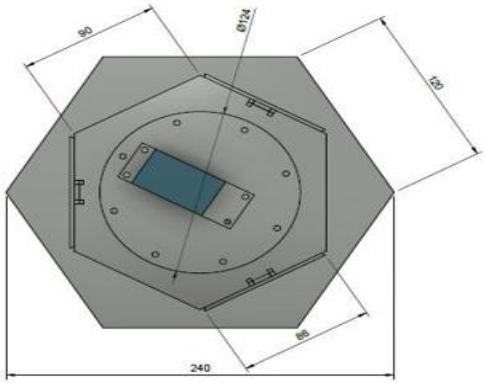

Fig 22 Top View.

Front View:

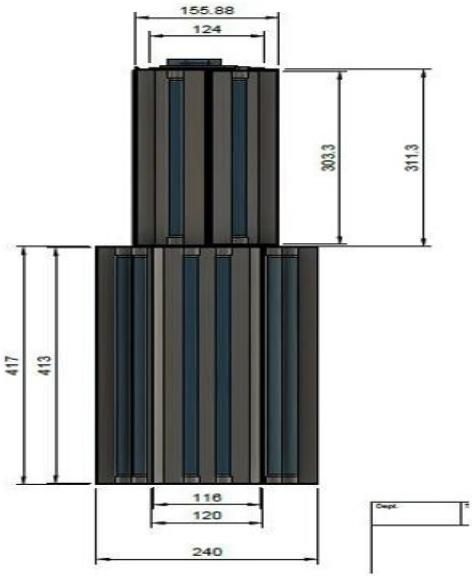

Fig 23 Front View.

4. Basel Assembly:

Top: Side View:

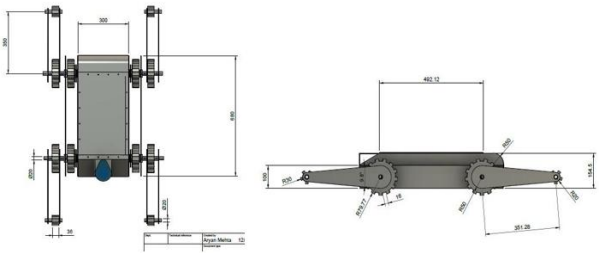

Fig 24 Top-view side-view

Isometric View

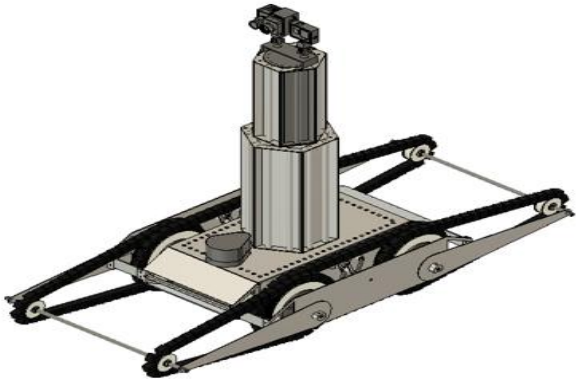

Fig 25 (View One)

Isometric View

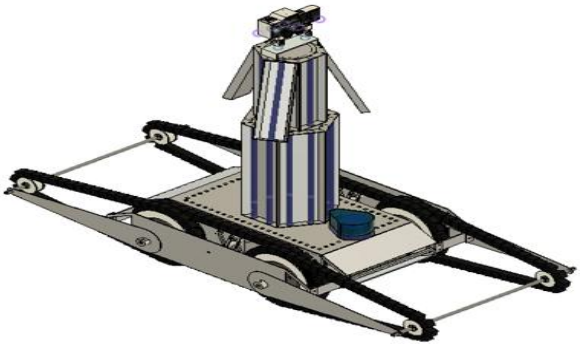

Fig 26 (View Two).

IX. CONCLUSION

The objective of designing a Autonomous UV Sanitization Robot with high safety and low production costs can be accomplished. The design is first conceptualized based on personal experiences and intuition. Engineering principles and design processes are then used to verify and create a Robot with optimal performance, safety, manufacturability, and ergonomics.
The design process included using Fusion 360 (Edu), Python Programming, software packages to model, simulate, and assist in the analysis of the completed Robot. After simulative tests, it is observed that our

design is easy to change and compatible with future upgrades. The compartmentalised aspects of the study have been integrated and applied to form a versatile solution to the current healthcare crisis. This design is able to eliminate the need for a human, to enter a microbiologically contaminated area to sanitize it. The utilitarian design can even be deployed in a public space to study the compliance of a population to social distancing and the wearing of masks. In the future this purpose driven autonomous robot will surely serve as an aid to humanity.

REFERENCES

[1] Ministry of Health & Family Welfare, "Advisory on Social Distancing Measure in the view of spread of COVID-19 disease", SocialDistancingAdvisorybyMOHFW.pdf, 2020.
[2] L. Hensley, "Social distancing is out, physical distancing is inheres how to do it," Global News–Canada (27 March 2020), 2020.
[3] Advanced Biotechnologies INC, "IS UV STERILIZATION EFFECTIVE FOR VIRUSES AND BACTERIA?" https://abionline.com/is-uv-sterilization-effective-for-viruses-and-bacteria/, December 8, 2020.
[4] Narinder Singh Punn, Sanjay Kumar Sonbhadra and Sonali Agarwal, "Monitoring COVID-19 social distancing with person detection and tracking via fine-tuned YOLO v3 and Deepsort techniques", 6 May 2020.
[5] S. K. Sonbhadra, S. Agarwal, and P. Nagabhushan, "Target specific mining of covid-19 scholarly articles using one-class approach," 2020.
[6] N. S. Punn and S. Agarwal, "Automated diagnosis of covid-19 with limited posteroanterior chest x-ray images using fine-tuned deep neural networks," 2020.
[7] N. S. Punn, S. K. Sonbhadra, and S. Agarwal, "Covid-19 epidemic analysis using machine learning and deep learning algorithms,"medRxiv, 2020. [Online]. Available: https://www.medrxiv.org/content/early/2020/04/11/2020.04.08.20057679.
[8] O. website of Indian Government, "Distribution of the novel coronavirus-infected pneumoniAarogyaSetu Mobile App," https://www.mygov.in/aarogya-setu-app/ , 2020.
[9] Robu.in, "RPLiDAR A1M8 360 Degree Laser Range Finder – 6m (Radius Range)", https://robu.in/product/rp-lidar-a1m8-360-degrees-laser-range-finder/
[10] Robu.in, "SHARP IR Distance Measuring Sensor Unit 4 ~ 30 cm With Cable-[GP2Y0A41SK0F]", https://robu.in/product/sharp-ir-distance-measuring-sensor-unit-4-30-cm-cable/ , 2020.
[11] Robu.in, "Orange 12V 300 RPM Johnson Geared DC Motor – Grade A Quality", https://robu.in/product/orange-12v-300-rpm-johnson-geared-dc-motor-grade-a-quality/ , 2020.
[12] Robu.in, "Orange MG555 12V 100RPM Square Gearbox DC motor For DIY Project", https://robu.in/product/orange-mg555-12v-100rpm-square-gearbox-dc-motor-for-diy-project/?gclid=EAIaIQobChMI_9ejk87M6wIVkg4rCh0hlQXbEAQYBCABEgJqkfD_BwE , 2020.
[13] Robu.in, "Cytron 10A Switch Control Potentiometer DC Motor Driver (MD10POT)", https://robu.in/product/cytron-10-a-switch-control-potentiometer-dc-motor-driver-md10pot/?gclid=EAIaIQobChMIu5P0idbM6wIV18EWBR16VQdFEAQYASABEgLeK_D_BwE , 2020.
[14] GIGABYTE, Mini-PC Barebone (BRIX), GB-BRi7H-10710 (rev. 1.0), https://www.gigabyte.com/in/Mini- PcBarebone/GB-BRi7H-10710-rev-10#kf , 2020.
[15] PHILIPS, Philips TUV 20W FAM TL Mini, https://www.vedgroup.net/products/philips-tuv-20w-fam-qty- 25-philipsuv?variant=535149645&currency=INR&utm_medium=product_sync&utm_source=google&utm_co ntent=sag_organic&utm_campaign=sag_organic&gclid=EAIaIQobChMI-bLOkKne6wIVQj5gCh0QrQxFEAYYASABEgIvRvD_BwE gh
[16] PHILIPS, Philips TUV 8W FAM TL Mini (1 Foot), https://www.vedgroup.net/products/philips-tuv-8w-fam-qty-25-philipsuv?variant=465248597&currency=INR&utm_medium=product_sync&utm_source=google&utm_ontent=sag_organic&utm_campaign=sag_organic&gclid=Cj0KCQjwpZT5BRCdARIsAGEX0zlqV894QdkbHNO mfQzAM67llbHUGJBYKg-CLqdp7m0U0E50hE8Yf_8aAlghEALw_wcB
[17] Electronics Tutorials, "Kirchhoff's Current Law", Home / DC Circuits / Kirchhoff's Current Law, https://www.electronics-tutorials.ws/dccircuits/kirchhoffs-current-law.html
[18] Jia-Wei Lin, Ming-Hung Lu, Yuan-Hsiang Lin, "A Thermal Camera based Continuous Body Temperature Measurement System", IEEE
[19] ImenHassani, ImenMaalej, and Chokri Rekik, "Robot Path Planning with Avoiding Obstacles in Known Environment Using Free Segments and Turning Points Algorithm", https://www.hindawi.com/journals/mpe/2018/2163278/
[20] Rajeev Chitguppi, Dental Tribune South Asia, https://in.dental-tribune.com/news/how-to-use-ultraviolet- light-uvc-to-fight-covid-19-effectively-in-dental-clinics-dr-ajay-bajaj, May 12, 2020.

About Author

[1] Aryan Mehta
Currently pursuing Bachelors of Technology (BTech) in Mechanical Engineering from VeermataJijabai Technological Institute, Matunga, Mumbai.
Email: aryanmehta2610@gmail.com, Mo: +91 9920833383
[2] Mohan Kshirsagar
Bachelors in Engineering (ENTC) from Sinhgad Institute of Technology Lonavala, currently working with On My Own Technology Pvt. Ltd. As Sr. Branch Manager, having 3 years of Experience in Robotics and STEM Education Email: k94mak@gmail.com, Mo: +91 9922879860.
[3] Reetu Jain Chiefmentor and Founder of On My OwnTechnology Private Limited Mumbai.
Web:www.onmyowntechnology.com,
Email:reetu.jain@onmyowntechnology.com, Mo: +91 9821137726.
[4] Shekhar Jain
Chief Executive Officer and Co-founder of On My Own Technology Private Limited Mumbai.
Web:www.onmyowntechnology.com,
Email:shekhar.jain@onmyowntechnology.com, Mo: +91 9820420629.